# Formation and Transport of Nanotube-Integrated Vesicles in a Lipid Bilayer Network

**Roger Karlsson,[†] Anders Karlsson,[†] and Owe Orwar*[,‡]**

*Department of Chemistry, Göteborg University, SE-41296 Göteborg, Sweden, and Department of Chemistry and Bioscience, and Microtechnology Centre at Chalmers, Chalmers University of Technology, SE-41296 Göteborg, Sweden*

*Received: February 27, 2003; In Final Form: August 6, 2003*

We present a micromanipulation method to create, load, and transport vesicles (with diameters of ∼500 nm to 5 $\mu$m) between two surface-adhered giant vesicles conjugated by a suspended nanotube. The walls of the lipid bilayer (two-dimensional liquid crystal) of the nanotube-integrated mobile vesicles are continuous with the nanotube walls and, thus, are 2-fold open-ended. Nanotube-integrated vesicles are created by the injection of excess membrane material into a surface-adhered vesicle. The transport of vesicles along the nanotubes is controlled using a difference in membrane tension that is caused by shape deformation of the surface-adhered vesicles using micromanipulator-controlled carbon fibers. When reaching a surface-adhered vesicle, a mobile vesicle can empty its contents into it on demand. This way, reactants or other chemical or physical cargo can be delivered into a neighboring vesicle to, for example, titrate a chemical substance or provide reactants to initiate a chemical reaction. This system is capable of controlled transport and handling of minute volumes ($10^{-12}$−$10^{-18}$ L), via manipulation of the energy state of the device material itself, and creates new possibilities for performing chemistry in aqueous phases at the nanoscale and microscale, as well as in the construction of nanofluidic devices.

## 1. Introduction

There is a steadily increasing interest in shrinking the size and volume of microfluidic systems toward the nanoscale. The small volume of nanofluidic systems could, for example, assist in bringing very interesting results and understandings in regard to how chemical reactions, e.g., enzyme catalysis, occur and how fluids behave in confined geometries.[1,2] These are highly relevant studies in regard to attempts to understand the chemistry in biological systems that occur on these length scales, as well as for a successful implementation and usage of chemistry in nanotechnological devices. In particular, for the characterization of single-molecule reactions, a constricted space and ultrasmall reaction volume are required to control and confine reactions (i.e., reaction initiation, diffusion and mixing times, and reactant concentrations), as well as having the capability to probe product formation using, for example, confocal laser-induced fluorescence microscopy[3] or microelectrochemistry.[4] However, the construction and operation of nanoscale fluidic devices presents daunting technological challenges. Fabrication of topologically complex three-dimensional nanoscale devices, using traditional silicon micromachining, is difficult, tedious, and expensive.[5] Also, the ability to transport materials and fluids with the needed precision is difficult, and until now, very few systems have been reported.[6] However, biological systems have many clever solutions to these problems, and instead of using hard and static systems, living cells use soft and dynamical materials to create nanofluidic systems that are able to sort, count, and perform chemical and physical operations on single molecules.[7]

We find inspiration in these biological systems, and we previously have described micromanipulation methods for creating networks of fluid-state bilayer vesicles and nanotubes that have controlled connectivity, geometry, topology, and chemistry.[8,9] Lipid material (the walls of the system), internal fluid, and particles can be transported throughout these nanotube−vesicle systems, using bilayer membrane flows that are controlled by differences in the surface free energy.[10] Here, a micromanipulation technique for the creation and transport of nanotube-integrated mobile vesicles is presented. These mobile vesicles are created on the suspended nanotubes that connect surface-adhered giant vesicles. They are formed by rapidly adding excess membrane material to one of the surface-adhered vesicles by merging it with another nanotube-connected vesicle. As a response to this perturbation, the nanotube that connects the surface-adhered vesicle increases its diameter severalfold and undergoes an asymmetrical shape change, first into a funnel-like geometry and then into a nanotube with integrated vesicles which are 2-fold open-ended (i.e., the walls of the vesicles are continuous with the walls of the nanotube). The conformation of nanotube−vesicle assemblies have been described previously in several other papers[11−16] and are commonly known as pearl-chain vesicles. However, these "pearling" states originate from different membrane energy states than those found in our starting system and also utilizes other excitational sources, such as optical tweezers,[14] the gradual disruption of the actin cytoskeleton,[13] or the anchoring of polymers to the membrane.[16]

The nanotubes in our system are suspended in solution and, therefore, the integrated vesicles created in our system are not attached to the underlying surface. This condition enables us to move the vesicles reversibly (back and forth) between the two surface-immobilized vesicles by controlling the direction of the difference in membrane tension. We also show that mobile vesicles can be made to coalesce and release their contents into one of the surface-immobilized vesicles on demand by increasing the surface tension of a target vesicle. Consequently, we

* Author to whom correspondence should be addressed. E-mail: orwar@phc.chalmers.se.
[†] Göteborg University.
[‡] Chalmers University of Technology.

10.1021/jp034502l CCC: $25.00 
Published on Web 09/12/2003

have created a system that is capable of transporting minute volumes ($10^{-18}$−$10^{-12}$ L) of liquid to target containers in the confines of a single bilayer membrane. This may lead to progress and development of a new class of biomimetic nanofluidic devices that operate by manipulation and control of the physical state of the device material itself. This technique of using a two-point perturbation, by changing the surface tension ($\sigma$) in membrane-lipid donor and acceptor vesicles also is the foundation for creating a nanofluidic device (or nanoscale valve) for large-scale network integration.[17]

## 2. Materials and Methods

**2.1. Chemicals.** Trizma base, glycerol, and potassium phosphate ($K_3PO_4$) were obtained from Sigma−Aldrich Sweden AB. Soybean lecithin (SBL, a polar lipid extract) was obtained from Avanti Polar Lipids, Inc. (700 Industrial Park Drive, Alabaster, AL 35007). Chloroform, EDTA (titriplex III), magnesium sulfate ($MgSO_4$), potassium dihydrogen phosphate ($KH_2PO_4$), potassium chloride, sodium chloride, and magnesium chloride were obtained from VWR International (Göteborg, Sweden). Deionized water from a Milli-Q system (Millipore Corp., Bedford, MA) was used to prepare the buffers. Green fluorescent 30-nm fluospheres, 505/515, and fluorescent dextrane were obtained from Molecular Probes (Leiden, The Netherlands).

**2.2. Formation of Giant Vesicles.** Vesicles were prepared from SBL, which was dissolved in chloroform (typically 100 mg/mL) as stock solution. The SBL lipids that were used consisted of a mixture of phosphatidylcholine (45.7%), phosphatidylethanolamine (22.1%), phosphatidylinositol (18.4%), phosphatidic acid (6.9%) and other compounds (6.9%). (The polar lipid extract composition was obtained from Avanti Polar Lipids, Inc.) To make unilamellar liposomes, a dehydration/rehydration technique that has been described by Criado and Keller[18] was used, with modifications.[19] The method is known to produce not only unilamellar but also multilamellar vesicles (MLVs). Briefly, 30 $\mu$L of a 100 mg/mL solution of SBL in chloroform was placed in a 10-mL round flask that also contained 200 $\mu$L of additional chloroform. The chloroform was removed by rotaevaporating the solution (under reduced pressure and at room temperature) for at least 4 h, and a dry lipid film was created. Buffer solution (Trizma base, 5 mM; $K_3PO_4$, 30 mM; $KH_2PO_4$, 30 mM; $MgSO_4$, 1 mM; and ethylenediaminetetraacetic acid (EDTA), 0.5 mM; pH 7.8, 3 mL) was carefully added to the round flask to swell the lipid film. The solution was placed in a refrigerator overnight. Glycerol (1 vol %) was added to the round flask, and the solution was placed in an ultrasonic bath for 15 min, forming an opaque lipid dispersion that contained 1 mg of lipid/(mL of solution). To form the unilamellar vesicles, 5 $\mu$L of the lipid dispersion was placed on a cover slip glass and the solution was then dehydrated in a vacuum desiccator. When the lipid film was completely dry, it was carefully rehydrated with buffer again (using the same buffer solution as that previously noted) to swell the lipid film. After a few minutes, giant unilamellar vesicles (GUVs) were formed.[19]

**2.3. Microscopy and Micromanipulation.** Rectangular cover slip glasses (No. 1) with liposome suspension were placed directly on the microscope stage of an inverted microscope (Leica DM IRB, Wetzlar, Germany) that was equipped with a Leica PL Fluotar 40× and PL APO 63× objective. Bright-field images were captured by a charge-coupled device camera (Hamamatsu Photonics Norden AB, Solna, Sweden), and an Argus-20 image processor was used as a real-time image enhancer. Recordings were performed using a Super VHS recorder (25 Hz frame collection rate; Panasonic S-VHS AG-5700, Stockholm, Sweden).

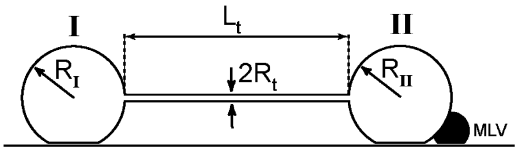


**Figure 1.** Schematic drawing of the starting system consisting of two surface-adhered giant vesicles interconnected by a nanotube. Surface-adhered vesicles are denoted as **I** and **II** and had a typical radii $R_I$ and $R_{II}$ of 10 $\mu$m. Nanotubes had a typical length of $L_t \approx 30$ $\mu$m and a radius of $R_t \approx 100$ nm. Networks were produced via a microinjection technique,[9] and a multilamellar protrusion (MLV), here depicted at vesicle **II**, was attached to the unilamellar system. The function of the MLV is to provide lipid material to the unilamellar system during construction and operation of the networks.

**2.4. Formation of Networks.** The networks were constructed using a microelectroinjection technique that has been described elsewhere.[9] When constructing large networks, a multilamellar protrusion attached to the unilamellar system is crucial for providing enough lipid material. The MLV feeds lipid material into the system, thereby buffering the surface tension. The electroinjections were controlled by a microinjection system (Eppendorf Femtojet, Hamburg, Germany) and a pulse generator (Digitimer Stimulator DS9A, Welwyn Garden City, U.K.). The injection tips used for formation of the networks were prepared from borosilicate capillaries (product GC100TF-10, Clark Electromedical Instruments, Reading, U.K.). A $CO_2$-laser puller (model P-2000, Sutter Instrument Co. Novato, CA) was used to create the injection tips. Carbon-fiber microelectrodes (5 $\mu$m in diameter, product ProCFE; Dagan Corporation, Minneapolis, MN) were used as counter electrodes.

**2.5 Theory.** The starting point of the experiments was a system of two surface-adhered giant vesicles, which are denoted as **I** and **II**, connected by a suspended nanotube (Figure 1). Vesicle **II** is connected to a MLV, which functions as a lipid reservoir. For the experiments, systems were prepared where the surface-adhered vesicles had radius sizes of ∼10 $\mu$m and the nanotubes had a radius of ∼100 nm and a length of ∼30 $\mu$m.

The geometrical shape of the system of vesicles and nanotubes can be found by minimizing the elastic energy, $E$:

$$E = \frac{k_c}{2}\int (2K - K_0)^2 \, dS + \int \sigma \, dS - WA_c \qquad (1)$$

where $k_c$ is the bending elasticity modulus of the lipid bilayer and $K$ and $K_0$ are the mean and spontaneous curvatures, respectively, of the lipid bilayer. The membrane tension is denoted as $\sigma$, $S$ is the surface area of the entire system, $A_c$ is the contact area of the surface-adhered vesicles, and $W$ is the contact potential. The first term represents Helfrich's curvature elasticity, the second term corresponds to the tension of the membrane, and the third term corresponds to the adhesion of the vesicles to the underlying surface. Another factor that will influence the energy of the system is the MLV that is attached to vesicle **II** (see Figure 1). The MLV can feed lipid material into the unilamellar system and thereby reduce the tension and reduce the energy.

The system is constructed from a continuous lipid bilayer; therefore, the shape that has the least energy is a sphere. However, by point-attaching the nanotube-conjugated vesicles onto a surface, the spherical configuration cannot be obtained. The shape of the system will instead be determined by a balance between the bending, tension, and adhesion energies, which

favors a system of near-spherical surface-adhered vesicles that are connected by thin tubes. Geometrical considerations indicate that the membrane in the tube segment will be at a higher energy state, compared to the surface-adhered vesicles, because of a greater contribution from the bending energy. The energy of the tube, $E_{tube}$, can be derived from the aforementioned Helfrich equation, and one obtains

$$E_{tube} = \left(\frac{k_c}{2R_t^2} + \sigma\right) 2\pi R_t L_t \qquad (2)$$

where $R_t$ and $L_t$ are the radius and length of the nanotube, respectively. Any spontaneous curvature has been neglected in this formula.[20] By taking the partial derivative of $E_{tube}$, with respect to $R_t$ ($\delta E_{tube}/\delta R_t$), and setting this variable to zero, the equilibrium radius $R_{t0}$ of the tube can be found as

$$R_{t0} = \sqrt{\left(\frac{k_c}{2\sigma}\right)} \qquad (3)$$

This relation shows that the tension $\sigma$ works to reduce the radius of the nanotube $R_t$, whereas the bending elasticity modulus ($k_c$) wants to increase it. This has been proven in solitary vesicles using tether pulling experiments, showing that there is an inverse relationship between membrane tension and tube radius.[21] The entire system demonstrates a pronounced fluidity; therefore, the stability of the system can be disturbed by changing the value of $\sigma$, which is competing with the curvature of the membrane.

## 3. Results and Discussion

**3.1. Formation of Networks and Nanotube-Integrated Vesicles.** Networks that consisted of two surface-adhered giant vesicles (denoted as **I** and **II** in Figure 1) conjugated by a suspended nanotube (see Figures 1 and 2a) were produced using a previously described micromanipulation method.[9] In brief, a borosilicate microinjection tip filled with buffer solution was inserted into a MLV-connected unilamellar vesicle, and after the lipid had sealed around the tip, it was pulled out of the vesicle, whereby a nanotube was formed. By injecting buffer into the nanotube orifice, a new vesicle was created by taking lipid material from the original vesicle (and the MLV) across the nanotube. After the new vesicle had reached a desired size, it was moved using the micromanipulator-controlled injection tip and allowed to attach to the surface. Using this technique for the formation of networks, fluid contact is established between the containers and the system is made from a continuous lipid wall. The success rate for forming these networks was almost 100%,[9] and the time required to construct a network of two vesicles interconnected by a lipid nanotube (when all the starting material is in place) was often <10 min. The networks were stable for hours, up to 24 h on a substrate whose interactions with the lipid material were neither too high nor too low.

To create the nanotube-integrated vesicles, we developed a two-point perturbation technique in which the surface tension was decreased in one of the surface-adhered GUVs while it was increased at the other GUV. To decrease the surface tension in a surface-adhered GUV by injection of surplus membrane material, a new vesicle (**III**) was formed, which was connected to the GUV by a nanotube, as shown schematically in Figure 2b and in the bright-field microscopy image in Figure 3a. Vesicles **I** and **III** could then be rapidly recombined by consuming the newly formed nanotube either by moving vesicle **III** to vesicle **I** or by increasing the size of vesicle **III** through

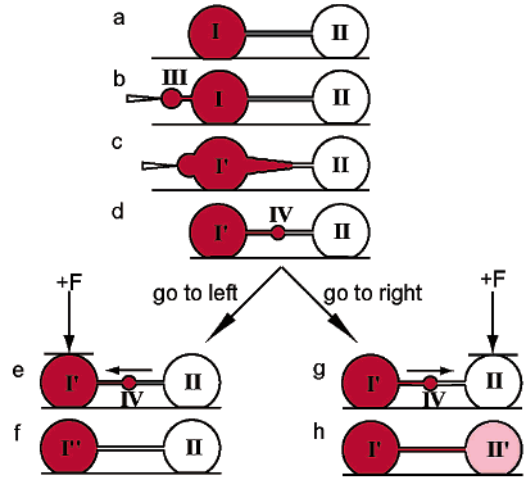


**Figure 2.** Schematic drawing showing the formation of nanotube-integrated mobile vesicles. Panel a shows the starting system of two nanotube-interconnected surface-adhered vesicles. In panel b, an injection tip (left) was inserted into vesicle **I**, using electroinjection, and a nanotube was pulled out. By injecting buffer into the nanotube orifice, a new daughter vesicle was formed, denoted here as **III**. Panel c shows that vesicle **III** grew to the desired size, taking membrane material from the system, originally coming from the multilamellar protrusion of vesicle **II** (not shown). Vesicle **III** was then allowed to remerge with vesicle **I**, thereby destabilizing it and the nanotube connected to it. The nanotube junction was dilated, and both fluid and membrane material were sampled from vesicle **I** and entered the funnel-like deformed nanotube. The volume and membrane area of vesicle **I** is changed, indicated by **I′**. Panel d shows that the system tried to minimize the elastic energy by reproducing two surface-adhered vesicles interconnected by a nanotube. Because excess fluid and membrane material had entered the deformed nanotube, small mobile vesicles (**IV**) were formed instead, integrated onto the nanotube, presumably all with the same composition as vesicle **I**. Panels e and f show that, by increasing the surface tension in vesicle **I′** through shape deformation, lipids will flow from regions of lower tension across the nanotubes to the point of perturbation and the mobile vesicles are transported along the flow. After the mobile vesicles reach the surface-adhered vesicle, they can inject their material into it. The remerging of the mobile vesicles again causes a change in the volume of the original vesicle **I**, denoted by **I″**. Panels g and h show that if, instead, the tension is increased in vesicle **II**, the mobile vesicles will move in the opposite direction and, in this case, the contents of vesicle **II** will be changed. The change in concentration, volume, and membrane area of this vesicle is indicated by **II′**.

buffer injection. In both cases, the close contact of the vesicles leads to rapid expansion of the nanotube and recombination of vesicle **III** with vesicle **I**. This is similar to fusing together two solitary spherical vesicles, and the area:volume ratio of the "product" vesicle will increase and result in a surplus of membrane material. The "product" vesicle will therefore not be spherical. This phenomenon can be used to establish a local and momentary reduction of the tension in a system of nanotube-interconnected vesicles. Fusion of a solitary vesicle to a network or combination of two nanotube-connected vesicles are two possible ways of performing this reduction. Earlier work on deflated vesicles mention a 3% excess area limit for stable vesicle shapes (ellipsoids).[22] Above this limit, free vesicles have a tendency to expel the redundant area, and, in our case, the nanotube seems to work as a drain for this excess membrane, because of the suddenly formed tension difference between vesicles **I** and **II** and the higher energy state of the nanotube. By the sudden addition of excess membrane material, both vesicle **I′** and the nanotube connected to the other surface-adhered GUV were momentarily destabilized (see Figures 2c and 3b). The junction between the GUV with excess membrane

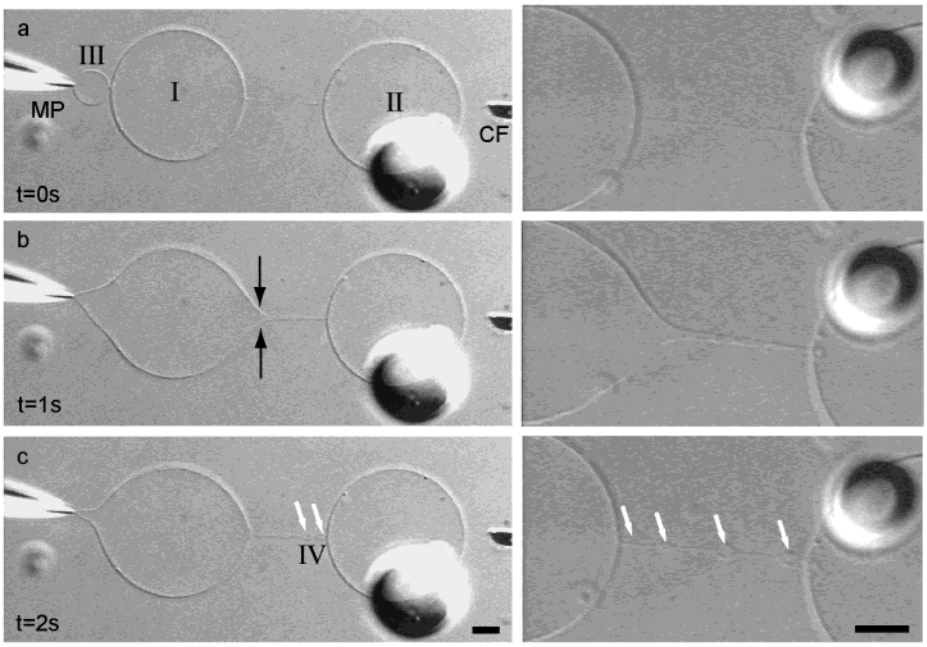


**Figure 3.** Photomicrographs (DIC optics) showing time-sequences of the formation of nanotube-integrated mobile vesicles. Images on the left-hand side depict the entire system, which consists of the unilamellar vesicles **III**, **I**, and **II**; also shown are the micropipet (MP) and the carbon fiber (CF) used for the creation of the system and the multilamellar protrusion (MLV) attached to vesicle **II**. Right-hand side of the figure shows magnified views of the nanotube region during formation of the mobile vesicles, corresponding to the left sequence (note that the enlargement is from an experiment different from the first sequence). Panel a shows that the starting system consisted of a network of three unilamellar vesicles interconnected by nanotubes, as described in Figure 2. The two giant vesicles, **I** and **II**, were attached to the surface, whereas vesicle **III** (left-hand side) was attached to the pipet. Panel b shows that, when vesicles **III** and **I** were allowed to remerge, the nanotube−vesicle junction of vesicle **I** was opened and both lipid and fluid flowed into the nanotube (from left to right). Panel c shows that the system tried to minimize the elastic energy by reproducing the nanotube. However, because of the excess fluid that was trapped inside the deformed nanotube, vesicles (**IV**) were formed instead (white arrows). Typical times for the different stages are indicated in panels a, b, and c, respectively. In this case, a continuous injection was performed and, as shown in the figure, buffer was eluted from the micropipet, reforming the micropipet-attached vesicle shown in panel a after the system had stabilized and returned to the original shape of surface-adhered vesicles with an interconnecting nanotube. Scale bar represents 10 $\mu$m.

material and the nanotube was dilated and both membrane material and internal fluid flowed into the deformed nanotube. This can be explained by the aforementioned eq 1 by noticing that bending will dominate, which subsequently leads to an increase in the diameter of the thin tubes. Typically, tube diameters grew up to 10-fold (from ~0.2 $\mu$m to 2 $\mu$m) at the largest-diameter position of the tube.

The excess-membrane system with a dilated nanotube vesicle is energetically unstable, and it strives to minimize its energy, by creating a system of two surface-adhered vesicles that are conjugated by a nanotube. The spherical shape of the surface-adhered vesicle injected with excess membrane is re-established within seconds and membrane material flows from the deformed nanotube to the surface-adhered vesicles. Because internal fluid has entered the deformed nanotube, the volume is too large to be accommodated by the nanotube simply by an isotropic dilation, which leads to diameter increase, because of the energetic constraints set by eq 2. Instead, undulations or varicosities on the destabilized nanotube therefore transform to vesicular structures that are denoted as **IV** in Figure 2 (see Figures 2d and 3c). This transformation is usually completed within a few seconds, as indicated in Figure 3. Because of the fact that the system consists of a continuous lipid wall, the small vesicles are thus integrated into the suspended nanotube with both ends open. Another interesting observation is that only one of the GUV−nanotube junctions opens when material is added, namely the end that is connected to the vesicle that is receiving excess material (see Figures 2c and 3b). This observation means that all of the fluid, which moves into the deformed nanotube during destabilization, originates from vesicle **I** and the content of the mobile vesicle formed onto the nanotube is, therefore, the same as (or very similar to) that of vesicle **I**. After formation, the nanotube-integrated vesicles were stable on the nanotube during the time course of the succeeding transport experiments, up to hours.

**3.2. Transport of Vesicles Loaded with Nanoparticles and Controlling the Transport Direction of Vesicles.** It was possible to transport nanotube-integrated vesicles to either one of the surface-adhered vesicles, **I** and **II**, into which they also could empty their contents on demand. The vesicle transport was based on inducing lipid flows by creating a tension difference across the lipid bilayer system. This was achieved using mechanical microprobes that were controlled by micromanipulators.[10] Using the microprobes to create a point force that acts on the membrane of one surface-adhered giant vesicle, the surface tension is increased locally and lipids will flow from regions of lower tension to the point of higher tension. We have previously used this type of surface free-energy control for the transport of lipid, fluid, and particles,[7] and this phenomenon is also crucial for construction of the networks, because the newly formed vesicles are taking lipid material from the rest of the network during growth.[9] Lipid velocities of up to 100 $\mu$m/s could be achieved and, therefore, the transport of the mobile vesicles between the surface-adhered vesicles could be performed within seconds.

We used a continuous-flow injection system, where buffer solution was constantly flowing at a low rate (typically tens of femtoliters per second) from the micropipet tip sealed to the nanotube. Thereby, a new daughter vesicle (**III**) was repeatedly formed at the tip orifice by retrieving a portion of the excess

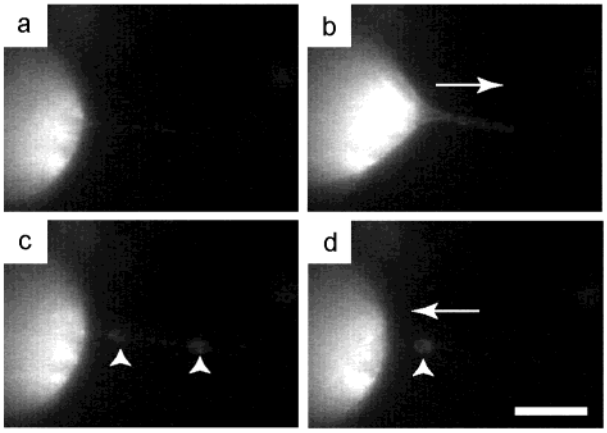


**Figure 4.** Fluorescence micrographs showing the formation and back transport of nanotube-integrated vesicles. Panel a shows vesicle **I**, which was filled with 30-nm-diameter fluorescent beads. Panel b shows that, when the system was destabilized by the remerging of vesicle **III** (not shown in the picture), the beads followed the flow (white arrow) of the fluid and migrated into the nanotube. Panel c shows that two vesicles integrated on the nanotube were formed, enclosing several beads (noted by white arrowheads). Panel d shows that a continuous injection of buffer was performed. By injecting buffer into vesicle **I** after the remerging of vesicles **III** and **I**, the membrane tension of vesicle **I** could be increased and the flow of lipid was reversed (white arrow), whereby the mobile vesicles started to move toward it, following the induced lipid flow. Mobile vesicles were transported to vesicle **I**, and one of them remerged with it, thereby releasing the beads into it. Scale bar represents 10 $\mu$m.

membrane material. This repetitive vesicle formation, in turn, leads to a repetitive formation of nanotube-integrated vesicles (formed when vesicle **I** has excess membrane), as well as their repetitive transport back to vesicle **I** (caused by lipid flow induced by the continuously growing vesicle **III**). One cycle of this process is illustrated in the series of fluorescence micrographs displayed in Figure 4, where panel a shows a partial image of two surface-adhered vesicles conjugated by a suspended nanotube. Vesicle **I** contained 30-nm-diameter green-fluorescent latex beads. A small vesicle (**III**) that contained beads was then created from the system and rapidly back-injected into vesicle **I**, resulting in a junction opening and tube dilation (see Figure 4b). Fluid and the 30-nm-diameter beads flowed into the nanotube and a nanotube-integrated vesicle (**IV**) was formed (see Figure 4c) that had the same composition as vesicle **I**.

Back injection of the nanotube-integrated vesicles into vesicle **I** is shown in Figure 4d. This occurs as a function of membrane transport that is induced by the continuous injection of buffer into vesicle **III**, which grows by taking lipid material from the system, as described previously. This continuous injection of buffer to the nanotube orifice to grow vesicles results in faster removal of the excess membrane area in the tube.

The propagation of a mobile vesicle, and its velocity along the nanotube, is determined primarily by the difference in membrane tension across the nanotube and the effective viscosity of the system, $\eta$:

$$v = \frac{\Delta\sigma}{\eta} \tag{4}$$

where $\eta$ is dependent on the viscosity of the lipid, the viscosity of the medium that surrounds the lipid, the opposing Stokes drag exerted on the mobile vesicles by the surrounding medium, intermonolayer friction,[23] and possible slipping between the lipid and the water inside the mobile vesicles.[24] Noticeably, eq 4 is a generalization of the work done by Chizmadzhev et al.[25]

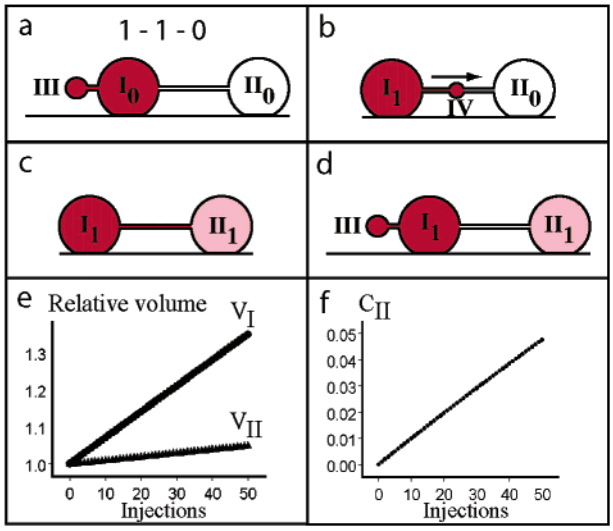


**Figure 5.** Schematic drawing showing a hypothetical titration situation. Panel a shows the system, which consists of three interconnected vesicles: one pipet-attached vesicle (**III**) and two surface-adhered vesicles (**I** and **II**). The system was named 1-1-0, because vesicles **III** and **I** had a unitary concentration of a certain substance and vesicle **II** had a zero concentration. Panel b shows that vesicle **III** was allowed to merge with vesicle **I**, and a nanotube-integrated vesicle (**IV**), which also had a unitary concentration, was formed. The volume of vesicle **I** was changed, which was denoted by $\mathbf{I}_1$, where the subscript indicates that this was the first remerging between the pipet-attached vesicle **III** and the surface-adhered vesicle **I**. In panel c, vesicle **IV** was made to merge with vesicle **II**, whereby the contents were released and the concentration was increased. The change in volume and concentration during this first injection was denoted by $\mathbf{II}_1$. Panel d represents a new starting system before the next cycle. Panel e shows plots of the relative volumes of vesicles **I** and **II** during the theoretical titration versus number of injections. The volume of vesicle **I** increased more rapidly, because it remerged with vesicle **III** (which had a radius of 2 $\mu$m) whereas vesicle **II** remerged with the smaller vesicle **IV** (which had a radius of 1 $\mu$m). Panel f shows the concentration of vesicle **II** during the theoretical titration versus number of injections. At every injection, a 1-$\mu$m-radius vesicle that had a unitary concentration was injected into vesicle **II** and the surface area, volume, and concentration of vesicle **II** was calculated. After 50 injections, the concentration was 0.05 units, starting at zero concentration. Any backflow of substance during the formation of a new vesicle **III** was neglected in the calculations.

Mobile vesicles can also be controlled in regard to transport in the other direction toward vesicle **II**. This is illustrated in Figure 2g−h. If the mobile vesicle merges with vesicle **II**, and releases its content into this container, we can deliberately change the fluid matrix of this surface-adhered vesicle in precise steps. A small volume of reagent can be added to a sample container to, for example, find the concentration of a substance (e.g., a titration experiment) and also to start reactions. This would create possibilities to perform chemistry in micrometer-diameter reactors by adding samples of volumes in the range of $10^{-18}$−$10^{-12}$ L. To explore this ability, we first considered a very simple hypothetical "titration", with the system illustrated in Figure 2b. The system **III**−**I**−**II** was named 1-1-0, where 1 or 0 denote containers that have a unitary concentration or zero concentration, respectively, of an arbitrary substance (see Figure 5a). The pipet-attached vesicle **III** was assumed to have a size of 2 $\mu$m in diameter, whereas the surface-adhered vesicles **I** and **II** were set to have a diameter of 10 $\mu$m.

Vesicles **III** and **I** were allowed to recombine, and we further assumed that this will produce one nanotube-integrated mobile vesicle, **IV**, with a diameter of 1 $\mu$m, of unit concentration (see Figure 5b). In case the contents of vesicles **III** and **I** are different, one must consider the diffusive and convective mixing

times during the recombination of the two vesicles, because this will influence the composition of vesicle **IV**. If vesicle **III** is much smaller than vesicle **I**, then convective mixing can be neglected and diffusion dominates. Therefore, vesicle **IV** will have the same concentration as that of vesicle **I**, before the recombination, because the time required for the system to regain its original shape of two surface-adhered vesicles connected by a nanotube (now with mobile vesicles) is shorter than the mixing time scale. If vesicles **III** and **I** are equally sized, however, convection will be more dominant and the concentration of vesicle **IV** is expected to be similar to the arithmetic mean of vesicles **I** and **III**.

After formation, the mobile vesicle was assumed to move to and release its content into the surface-adhered vesicle **II** (see Figure 5c). This cycle of events was then repeated several times. The change in the volume of vesicles **I** and **II**, as a function of the number of injections, can be explained by the following equations:

$$V(\mathbf{I}_n) = V(\mathbf{I}_{n-1}) + nV(\mathbf{III}) - nV(\mathbf{IV}) \quad (5)$$

$$V(\mathbf{II}_n) = V(\mathbf{II}_{n-1}) + nV(\mathbf{IV}) \quad (6)$$

where $n$ is the number of injections ($n = 1, 2, 3, ...$). The volume of vesicle **I** increases by the addition of vesicle **III**, but it also loses a small amount in the formation of the mobile vesicle **IV**.

The relative increase in the volume of vesicles **I** and **II**, with respect to the starting situation, was plotted (see Figure 5e), as well as the concentration of vesicle **II** (see Figure 5f). These figures show that the volume of vesicle **I** increases more rapidly than that of vesicle **II**, because the added vesicle **III** is twice as large as vesicle **IV**, which is made to remerge with vesicle **II**.

To illustrate this condition experimentally, vesicles **III** and **I**, but not vesicle **II**, were filled with fluorescent dextrane (1 mg/mL; see Figure 6a). After vesicle **III** remerged with vesicle **I**, a mobile vesicle was formed that contained the fluorescent dextrane solution. A micromanipulator-controlled carbon fiber was then used to deform vesicle **II**, which led to a momentary increase in the membrane tension, inducing a flow of lipid toward it,[10] which is schematically shown in Figure 2g−h. As mentioned previously, the mobile vesicles follow the lipid flow[24] and the increased tension also allows them to merge with vesicle **II**. Theoretically, it has been shown that the remerging of two vesicles interconnected by a short nanotube is facilitated by the sum of tension in the two vesicles.[25] This is consistent with our experiments, because stretching the membrane of vesicle **II** leads to greater success in the merging of the mobile vesicles. The cycle was repeated 40 times, which led to a buildup in the concentration of fluorescent dextrane in vesicle **II** (which had zero concentration of fluorescent dextrane at the starting point; see Figure 6b). It is important to realize that the volumes of this titration system are in the femtoliter to picoliter range ($10^{-15}$−$10^{-12}$ L), because mobile vesicles that have femtoliter-scale volumes (radius of 1−2 $\mu$m) are injected into surface-adhered vesicles with picoliter-scale volumes. This experiment demonstrates the unique control of the transport and mixing of ultralow volumes in confined geometries.

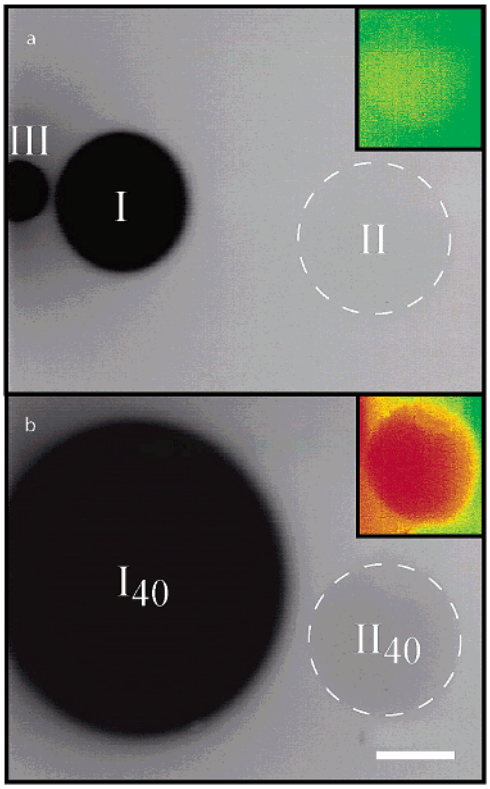


**Figure 6.** Fluorescence micrographs showing the injection of fluorescent dextrane into vesicle **II**. Fluorescent images were inverted to negative fluorescence to enhance the change in fluorescent intensity. Insets show a false-color-coded image of the fluorescence intensity of vesicle **II**. Both insets were digitally enhanced and processed in parallel. Starting system was the same as that in Figure 2b, which had fluorescent dextrane in vesicles **III** and **I**. A mobile vesicle was formed that had a diameter of ~2 $\mu$m. By shape deformation of vesicle **II**, as described in Figure 4 using a carbon fiber, a flow of membrane lipid was induced, forcing the mobile vesicle to move toward vesicle **II** and release its content. The injection procedure was repeated 40 times. Panel a shows the fluorescence intensity measurements of **II** before injecting any mobile vesicles have been injected, whereas panel b shows the final fluorescence intensity after 40 injections. As shown in Figure 5f, after 40 injections, only ~4% of the total volume was from the mobile vesicles that contained the fluorescent dextrane. Note the much-larger increase in the volume of vesicle **I** during the process. The large size of vesicle **I** also contributed to greater background fluorescence, compared to the starting conditions. The change in volume and concentration after 40 consecutive injections is indicated by $\mathbf{I}_{40}$ and $\mathbf{II}_{40}$. Scale bar represents 10 $\mu$m.

## 4. Conclusions

We have shown the formation and transport of submicrometer-sized vesicles integrated on lipid nanotubes that conjugate surface-adhered giant vesicles. A physical explanation for the formation and transport is also provided. We believe that the method of moving and remerging these nanotube-integrated vesicles will be important for the delivery, transport, and mixing of small packets of fluid. The volumes that are handled in the bilayer system are in the femtoliter to picoliter range ($10^{-18}$−$10^{-12}$ L), where mobile vesicles of femtoliter-scale volumes are transported between, and injected into, surface-adhered vesicles of picoliter-scale volumes. One example where this might be important is in the field of bioanalytical chemistry, where enzymatic reactions can be performed in the constricted and biomimetic environment that is provided by the bilayer membrane network. Vesicular transport along nanotubes is also a phenomenon that occurs in living cells, and, therefore, our fluidic networks might be used as a model system to give information about the transport mechanisms. Finally, it might also give inspiration to form new technological platforms to produce a novel class of microfluidic and nanofluidic devices that have the potential to work with single molecules and single nanoparticles.[10]

**Acknowledgment.** This work was supported by the Royal Swedish Academy of Sciences through a donation by the Wallenberg Foundation, the Swedish Research Council (VR), and the Swedish Foundation for Strategic Research (SSF). Professor Marina Voinova is acknowledged for fruitful discussions.

## References and Notes

(1) Chiu, D. T.; Wilson, C. F.; Ryttsén, F.; Strömberg, A.; Farre, C.; Karlsson, A.; Nordholm, S.; Gaggar, A.; Modi, B. P.; Moscho, A.; Garza-Lopez, R. A.; Orwar, O.; Zare, R. N. *Science* **1999**, *283*, 1892.

(2) Brody, J. P.; Yager, P.; Goldstein, R. E.; Austin, R. H. *Biophys. J.* **1996**, *71*, 3430.

(3) Nie, S. M.; Chiu, D. T.; Zare, R. N. *Science* **1994**, *266*, 1018.

(4) Fan, F. R. F.; Bard, A. J. *Science* **1995**, *267*, 871.

(5) de Boer, M. J.; Tjerkstra, R. W.; Berenschot, J. W.; Jansen, H. V.; Burger, G. J.; Gardeniers, J. G. E.; Elwenspoek, M.; van den Berg, A. *J. Microelectromech. Syst.* **2000**, *9*, 94.

(6) Knight, J. B.; Vishwanath, A.; Brody, J. P.; Austin, R. H. *Phys. Rev. Lett.* **1998**, *80*, 3863.

(7) Ishii, Y.; Yanagida, T. *Single Mol.* **2000**, *1*, 5.

(8) Karlsson, A.; Karlsson, R.; Karlsson, M.; Cans, A.-S.; Stromberg, A.; Ryttsen, F.; Orwar, O. *Nature* **2001**, *409*, 150.

(9) Karlsson, M.; Sott, K.; Cans, A.-S.; Karlsson, A.; Karlsson, R.; Orwar, O. *Langmuir* **2001**, *17*, 6754.

(10) Karlsson, R.; Karlsson, M.; Karlsson, A.; Cans, A.-S.; Bergenholtz, J.; Åkerman, B.; Ewing, A. G.; Voinova, M.; Orwar, O. *Langmuir* **2002**, *18*, 4186.

(11) Bar-Ziv, R.; Moses, E. *Phys. Rev. Lett.* **1994**, *73*, 1392.

(12) Nelson, P.; Powers, T.; Seifert, U. *Phys. Rev. Lett.* **1995**, *74*, 3384.

(13) Bar-Ziv, R.; Tlusty, T.; Moses, E.; Safran, S. A.; Berhadsky, A. *Proc. Natl. Acad. Sci. U.S.A.* **1999**, *96*, 10140.

(14) Bar-Ziv, R.; Moses, E.; Nelson, P. *Biophys. J.* **1998**, *75*, 294.

(15) Kosawada, T.; Skalak, R.; Schmid-Schönbein, G. W. *J. Biomech. Eng.* **1999**, *121*, 472.

(16) Tsafrir, I.; Sagi, D.; Arzi, T.; Guedeau-Boudeville, M.-A.; Frette, V.; Kandel, D.; Stavans, J. *Phys. Rev. Lett.* **2001**, *86*, 1138.

(17) Karlsson, R.; Karlsson, A.; Orwar, O. *J. Am. Chem. Soc.* **2003**, *125*, 8442.

(18) Criado, M.; Keller, B. U. *FEBS Lett.* **1987**, *224*, 172.

(19) Karlsson, M.; Nolkrantz, K.; Davidson, M. J.; Stromberg, A.; Ryttsen, F.; Akerman, B.; Orwar, O. *Anal. Chem.* **2000**, *72*, 5857.

(20) Derényi, I.; Jülicher, F.; Prost, J. *Phys. Rev. Lett.* **2002**, *88*.

(21) Evans, E.; Bowman, H.; Leung, A.; Needham, D.; Tirell, D. *Science* **1996**, *273*, 933.

(22) Evans, E.; Rawicz, W. *Phys. Rev. Lett.* **1990**, *64*, 2094.

(23) Evans, E.; Yeung, A. *Chem. Phys. Lipids* **1994**, *73*, 39.

(24) Goveas, J. L.; Milner, S. T.; Russel, W. B. *J. Phys. II* **1997**, *7*, 1185.

(25) Chizmadzhev, Y. A.; Kuzmin, P. I.; Kumenko, D. A.; Zimmerberg, J.; Cohen, F. S. *Biophys. J.* **2000**, *78*, 2241.